Partial Differential Equations

Mean Fields Games with congestion effects

TATOU DEKOU Thibault

1 Introduction and background

The theory of mean field games (MFGs) has been introduced in the pioneering works of J-M. Lasry and P-L. Lions [1, 2], and aims at studying deterministic or stochastic differential games (Nash equilibria) as the number of players tends to infinity. It supposes that the rational players are indistinguishable and individually have a negligible influence on the game, and that each individual strategy is influenced by some averages of quantities depending on the states (or the controls) of the other players. The applications of MFGs are numerous, from economics and finance to the study of crowd motion. On the other hand, very few MFG problems have explicit or semi-explicit solutions. Therefore, numerical simulations of MFGs play a crucial role in obtaining quantitative information from this class of models. In this project, the aim is to study numerical simulations of MFGs.

We start by supposing, for simplicity, that the state space is $\mathbb{R}^d$ so that no boundary conditions are needed. We fix a finite time horizon $T > 0$. Let $f : \mathbb{R}^d \times \mathbb{R} \times \mathbb{R}^d \to \mathbb{R}, \quad (x, m, \gamma) \mapsto f(x, m, \gamma)$ and $\varphi : \mathbb{R}^d \times \mathbb{R} \to \mathbb{R}, \quad (x, m) \mapsto \varphi(x, m)$ be respectively a running cost and a terminal cost, on which assumptions will be made later on. We consider the following MFG : find a flow of probability densities $\hat{m} : [0, T] \times \mathbb{R}^d \to \mathbb{R}$ and a feedback control $\hat{v} : [0, T] \times \mathbb{R}^d \to \mathbb{R}^d$ satisfying the following two conditions :

1. $\hat{v}$ minimizes

$$J_{\hat{m}}(v) = \mathbb{E}\left[\int_0^T f\left(X_t^v, \hat{m}(t, X_t^v), v(t, X_t^v)\right) dt + \varphi\left(X_T^v, \hat{m}(T, X_T^v)\right)\right] \tag{1}$$

subject to the constraint that the process $X^v = (X_t^v)_{t \geq 0}$ solves the stochastic differential equation (SDE)

$$dX_t^v = b(X_t^v, \hat{m}(t, X_t^v), v(t, X_t^v))dt + \sigma dW_t, \quad t \geq 0, \tag{2}$$

where σ is the volatility, b is a given function from $\mathbb{R}^d \times \mathbb{R} \times \mathbb{R}^d$ with values in $\mathbb{R}^d$, and X_0^v is an independent random variable in $\mathbb{R}^d$, distributed according to the law m_0.

2. For all $t \in [0, T]$, $\hat{m}(t, \cdot)$ is the law of $X_t^{\hat{v}}$. It is useful to note that for a given feedback control v, the density $m^v(t)$ of the law of X_t^v following (2) solves the Kolmogorov-Fokker-Planck (KFP) equation :

$$\begin{cases} \frac{\partial m_v}{\partial t}(t, x) - \nu \Delta m^v(t, x) + \operatorname{div}\left(m^v(t, \cdot) b(\cdot, \hat{m}(t, \cdot), v(t, \cdot))\right)(x) = 0, & \text{in } (0, T] \times \mathbb{R}^d, \\ m^v(0, x) = m_0(x), & \text{in } \mathbb{R}^d, \end{cases} \tag{3}$$

where $\nu = \frac{\sigma^2}{2}$.

Let $H : \mathbb{R}^d \times \mathbb{R} \times \mathbb{R}^d \to \mathbb{R}$ be the Hamiltonian of the control problem faced by an infinitesimal player. It is defined by

$$H(x, m, p) = \max_{\gamma \in \mathbb{R}^d} \left(-f(x, m, \gamma) - \langle b(x, m, \gamma), p \rangle \right).$$

In the sequel, we will assume that the running cost f and the drift b are such that H is well-defined, C^1 with respect to (x, p), and strictly convex with respect to p.

From standard optimal control theory, one can characterize the best strategy through the value function u of the above optimal control problem for a typical player, which satisfies a Hamilton-Jacobi-Bellman (HJB) equation. Together with the equilibrium condition on the distribution, we obtain that the equilibrium best response $\hat{v}$ is characterized by

$$\hat{v}(t, x) = \arg\max_{a \in \mathbb{R}^d} \left(-f(x, m(t, x), a) - \langle b(x, m(t, x), a), \nabla u(t, x) \rangle \right),$$

and, denoting H_p the gradient of H with respect to p, that the drift at equilibrium is

$$b(x, m(t, x), \hat{v}(t, x)) = -H_p(x, m(t, x), \nabla u(t, x)),$$

where (u, m) solves the following forward-backward PDE system :

$$\begin{cases} -\frac{\partial u}{\partial t}(t, x) - \nu \Delta u(t, x) + H(x, m(t, x), \nabla u(t, x)) = 0, & \text{in } [0, T) \times \mathbb{R}^d, \\ \frac{\partial m}{\partial t}(t, x) - \nu \Delta m(t, x) - \operatorname{div}\left(m(t, \cdot) H_p(\cdot, m(t, \cdot), \nabla u(t, \cdot)) \right)(x) = 0, & \text{in } [0, T) \times \mathbb{R}^d \\ u(T, x) = \varphi(x, m(T, x)), \quad m(0, x) = m_0(x), & \text{in } \mathbb{R}^d \end{cases} \tag{4}$$

We recall definitions of differential operators in $\mathbb{R}^d$. For a smooth function $\psi : \mathbb{R}^d \to \mathbb{R}$, let $\nabla\psi$ (the gradient of ψ) be the function $\nabla\psi : \mathbb{R}^d \to \mathbb{R}^d$ defined by $\nabla\psi(x) = \left(\frac{\partial \psi}{\partial x_1}(x), \ldots, \frac{\partial \psi}{\partial x_d}(x) \right)^T$ and let $\Delta\psi$ (the Laplacian of ψ) be the function $\Delta\psi : \mathbb{R}^d \to \mathbb{R}$ defined by $\Delta\psi(x) = \sum_{i=1}^d \frac{\partial^2 \psi}{\partial x_i^2}(x)$. For a smooth function $V : \mathbb{R}^d \to \mathbb{R}^d$, let $\operatorname{div}(V)$ (the divergence of V) be the function div(V) : $\mathbb{R}^d \to \mathbb{R}$ defined by $\operatorname{div}(V)(x) = \sum_{i=1}^d \frac{\partial V_i}{\partial x_i}(x)$. This work aims at studying models of MFG with congestion effects. The following section will give an idea of the subject.

2 A model of congestion

Consider the case where the drift is the control, i.e. $b(x, m, \gamma) = \gamma$, and the running cost is of the form $f(x, m, \gamma) = L_0(\gamma, m(x)) + f_0(x, m(x))$ where $L_0 : \mathbb{R}^d \times \mathbb{R}^+ \ni (\gamma, \mu) \mapsto L_0(\gamma, \mu) \in \mathbb{R}$

is given by

$$L_0(\gamma,\mu) = \frac{\beta-1}{\beta}(c_0+c_1\mu)^{\frac{\alpha}{\beta-1}}|\gamma|^{\frac{\beta}{\beta-1}},$$

where $\beta > 1$, $0 \le \alpha \le \frac{4(\beta-1)}{\beta}$, $c_0 \ge 0$, and $c_1 > 0$. The term $L_0(\gamma, m(x))$ models congestion effects, i.e. the fact that the cost of motion grows with the density of the population (the denser the population, the higher the cost of motion). Then

$$H(x,m,p) = \max_{\gamma\in\mathbb{R}^d}\{-L_0(\gamma,m(x)) - \langle\gamma,p\rangle\} - f_0(x,m(x)) = H_0(p,m(x)) - f_0(x,m(x)),$$

where

$$H_0(p,\mu) = \frac{1}{\beta}\frac{|p|^\beta}{(c_0+c_1\mu)^\alpha}.$$

In this situation, the best response at equilibrium is

$$\hat{v}(t,x,m) = -\frac{1}{(c_0+c_1m(t,x))^\alpha}|\nabla u(t,x)|^{\beta-2}\nabla u(t,x), \tag{5}$$

where (u,m) solves the PDE system

$$\begin{cases} -\frac{\partial u}{\partial t}(t,x) - \nu\Delta u(t,x) + \frac{1}{\beta}\frac{|\nabla u(t,x)|^\beta|}{(c_0+c_1m(t,x))^\alpha} = f_0(x,m(t,x)), & \text{in } [0,T)\times\mathbb{R}^d,\\ \frac{\partial m}{\partial t}(t,x) - \nu\Delta m(t,x) - \operatorname{div}\left(\frac{m(t,\cdot)}{(c_0+c_1m(t,\cdot))^\alpha}|\nabla u(t,\cdot)|^{\beta-2}\nabla u(t,\cdot)\right)(x) = 0, & \text{in } (0,T]\times\mathbb{R}^d,\\ u(T,x) = \varphi(x,m(T,x)), \quad m(0,x) = m_0(x), & \text{in } \mathbb{R}^d. \end{cases} \tag{6}$$

In this work, we will present a finite difference scheme first introduced in [3] to solve the special case of the above model of congestion. We suppose that $f_0(x,m(x)) = \tilde{f}_0(m(x)) + g(x)$. For simplicity, we focus on the one-dimensional setting, i.e., $d = 1$. We also suppose that the state space is the domain $\Omega =]0,1[$, i.e., the stochastic process involved in the dynamics of the players is reflected at $\partial\Omega$. The boundary value problem becomes

$$\begin{cases} -\frac{\partial u}{\partial t}(t,x) - \nu\frac{\partial^2 u}{\partial x^2}(t,x) + \frac{1}{\beta}\frac{\left|\frac{\partial u}{\partial x}(t,\cdot)\right|^\beta}{(c_0+c_1m(t,x))^\alpha} = g(x) + \tilde{f}_0(m(t,x)), & \text{in } [0,T)\times\Omega,\\ \frac{\partial m}{\partial t}(t,x) - \nu\frac{\partial^2 m}{\partial x^2}(t,x) - \frac{\partial}{\partial x}\left(\frac{m(t,\cdot)}{(c_0+c_1m(t,\cdot))^\alpha}\left|\frac{\partial u}{\partial x}(t,\cdot)\right|^{\beta-2}\frac{\partial u}{\partial x}(t,\cdot)\right)(x) = 0, & \text{in } (0,T]\times\Omega,\\ \frac{\partial u}{\partial x}(t,0) = \frac{\partial u}{\partial x}(t,1) = 0, & \text{on } (0,T),\\ \frac{\partial m}{\partial x}(t,0) = \frac{\partial m}{\partial x}(t,1) = 0, & \text{on } (0,T).\\ u(T,x) = \varphi(x,m(T,x)), \quad m(0,x) = m_0(x), & \text{in } \Omega. \end{cases} \tag{7}$$

3 Finite difference schemes

Let N_T and N_h be two positive integers. We consider N_T+1 and N_h points in time and space, respectively. Set $\Delta t = \frac{T}{N_T}, \quad h = \frac{1}{N_h-1}, \quad t_n = n \times \Delta t, \quad x_i = i \times h \quad$ for $(n,i) \in \{0,\dots,N_T\} \times \{0,\dots,N_h-1\}$. We approximate u and m respectively by vectors U and $M \in \mathbb{R}^{(N_T+1)\times N_h}$, that is, $u(t_n,x_i) \approx U_i^n, \quad m(t_n,x_i) \approx M_i^n \quad$ for each $(n,i) \in \{0,\dots,N_T\} \times \{0,\dots,N_h-1\}$. We use a superscript and a subscript, respectively, for the time and space indices. To take into account Neumann boundary conditions, we introduce ghost nodes $x_{-1} = -h, \quad x_{N_h} = 1+h$, and set $U_{-1}^n = U_0^n, \quad U_{N_h}^n = U_{N_h-1}^n, \quad M_{-1}^n = M_0^n, \quad M_{N_h}^n = M_{N_h-1}^n$.

3.1 Finite Difference Operators

We introduce the finite difference operators :

$$\begin{cases} (D_t W)^n = \frac{1}{\Delta t}(W^{n+1} - W^n), & n \in \{0,\dots,N_T-1\}, \quad W \in \mathbb{R}^{N_T+1}. \\ (DW)_i = \frac{1}{h}(W_{i+1} - W_i), & i \in \{0,\dots,N_h-1\}, \quad W \in \mathbb{R}^{N_h}. \\ (\Delta_h W)_i = -\frac{1}{h^2}(2W_i - W_{i+1} - W_{i-1}), & i \in \{0,\dots,N_h-1\}, \quad W \in \mathbb{R}^{N_h}. \\ [\nabla_h W]_i = ((DW)_i, (DW)_{i-1}) \in \mathbb{R}^2, & i \in \{0,\dots,N_h-1\}, \quad W \in \mathbb{R}^{N_h}. \end{cases}$$

For the special cases $i=0$ and $i=N_h-1$, we use the above-mentioned discrete version of the Neumann boundary conditions. Let $\tilde{H} : \mathbb{R}\times\mathbb{R}\times\mathbb{R}^+ \to \mathbb{R}, (p_1,p_2,\mu) \mapsto \tilde{H}(p_1,p_2,\mu)$ be a discrete Hamiltonian. It is defined by :

$$\tilde{H}(p_1,p_2,\mu) = \frac{\left((p_1)_-^2 + (p_2)_+^2\right)^{\frac{\beta}{2}}}{\beta(c_0+c_1\mu)^\alpha}$$

where X_+ and X_- stand for the positive and negative parts of X, respectively : $X = X_+ - X_-, \quad |X| = X_+ + X_-$, and we set $X_+^2 = (X_+)^2, \quad X_-^2 = (X_-)^2$.

Using these finite difference operators we will write the discrete version of the Hamilton Jacobi Bellman equation (HJB equation) and the Kolmogorov Fokker Planck equation (KFP equation in short) which are the two first equation in (7).

3.2 Discrete HJB equation

We consider the following discrete version of the HJB equation (First equation in (7) supplemented with the Neumann conditions and the terminal condition :

$$\begin{cases} -(D_tU_i)^n - \nu(\Delta_h U^n)_i + \tilde{H}([\nabla_h U^n]_i, M_i^{n+1}) = g(x_i) + \tilde{f}_0(M_i^{n+1}), & 0 \le i < N_h, \quad 0 \le n < N_T, \\ U_{-1}^n = U_0^n, & 0 \le n < N_T, \\ U_{N_h}^n = U_{N_h-1}^n, & 0 \le n < N_T, \\ U_i^{N_T} = \phi(M_i^{N_T}), & 0 \le i < N_h. \end{cases} \tag{8}$$

This scheme is an implicit Euler scheme since the equation is backward in time. To solve the HJB equation, we rewrite the first equation of the above system in the form $F(U^n, U^{n+1}, M^{n+1}) = 0$. We observe that by replacing the finite difference operators by their values we obtain :

$$\begin{cases} -\frac{U_i^{n+1} - U_i^n}{\Delta t} - \nu \frac{U_{i-1}^n - 2U_i^n + U_{i+1}^n}{h^2} + \frac{1}{\beta}\left(\left(\frac{U_{i+1}^n - U_i^n}{h}\right)_-^2 + \left(\frac{U_i^n - U_{i-1}^n}{h}\right)_+^2\right)^{\frac{\beta}{2}} \frac{1}{(c_0 + c_1 M_i^{n+1})^\alpha} = g(x_i) + f_0(M_i^{n+1}). \end{cases}$$

Using vectors, this becomes :

$$\begin{cases} F(U^n, U^{n+1}, M^{n+1}) := \frac{U^{n+1} - U^n}{\Delta t} + \kappa A U^n - (\beta(c_0 + c_1 M^{n+1})^\alpha)^{-1}\left(\left(\frac{D_{curr}U^n}{h}\right)_-^2 + \left(\frac{D_{past}U^n}{h}\right)_+^2\right)^{\frac{\beta}{2}} \\ +g(x) + f_0(M^{n+1}) = 0 \end{cases}$$

where $\kappa := \frac{\nu}{h^2}$ and the squarred matrix (order N_h) of finite difference operators D_{curr}, A and D_{past} are defined by :

$$A = \begin{bmatrix} -1 & 1 & 0 & \cdots & 0 \\ 1 & -2 & 1 & \cdots & 0 \\ 0 & 1 & -2 & \cdots & 0 \\ \vdots & \vdots & \vdots & \ddots & 1 \\ 0 & 0 & 0 & 1 & -1 \end{bmatrix}, \quad D_{\text{curr}} = \begin{bmatrix} -1 & 1 & 0 & \cdots & 0 \\ 0 & -1 & 1 & \cdots & 0 \\ 0 & 0 & -1 & \cdots & 0 \\ \vdots & \vdots & \vdots & \ddots & 1 \\ 0 & 0 & 0 & 0 & 0 \end{bmatrix}, \quad D_{\text{past}} = \begin{bmatrix} 0 & 0 & 0 & \cdots & 0 \\ -1 & 1 & 0 & \cdots & 0 \\ 0 & -1 & 1 & \cdots & 0 \\ \vdots & \vdots & \vdots & \ddots & 0 \\ 0 & 0 & 0 & -1 & 1 \end{bmatrix}$$

The Neumann conditions $U_{-1}^n = U_0^n$ et $U_{N_h}^n = U_{N_h-1}^n$ justify the values of the first and the last element of the above matrix. In order to solve a linear system of the form $F(U^n, U^{n+1}, M^{n+1}) = 0.$, one may use the Newton Raphson algorithm which at each iteration is about to update the solution like this : $U^{n,k+1} = U^{n,k} - J^{-1}(U^{n,k}, U^{n+1}, M^{n+1})F(U^{n,k}, U^{n+1}, M^{n+1})$. Starting from the terminal time step N_T for which the left hand of the last equation in (7) gives an explicit formula for U^{N_T}, the backward loop consists of computing U^n by solving the Discrete HJB equation given U^{n+1} and M^{n+1}. For implementation, one may choose the initial guess $U^{n,0} = U^{n+1}$. The Newton iterations are stopped when the residual $\|F(U^{n,k}, U^{n+1}, M^{n+1})\|$ is smaller than a given threshold, say 10^{-10}. By the iterations sequence, we see that we need to compute the jacobian matrix of F at U^n defined by : $J_{ij} = \frac{\partial F_i}{\partial U_j^n}$. Since the expression of F only depends on $U_{i-1}^n, U_i^n, U_{i+1}^n$, so the Jacobian is a tridiagonal matrix. Moreover :

$$\frac{\partial F_i}{\partial U_{i-1}^n} = \frac{\nu}{h^2} + \frac{1}{h(c_0+c_1 M_i^{n+1})^\alpha}\frac{(U_i^n - U_{i-1}^n)}{h} + (\frac{(U_{i+1}^n - U_i^n)_-^2}{h} + \frac{(U_i^n - U_{i-1}^n)_+^2}{h})^{\beta/2-1}$$

$$\frac{\partial F_i}{\partial U_i^n} = -\frac{1}{\Delta t} - \frac{2\nu}{h^2} - \frac{1}{h(c_0+c_1 M_i^{n+1})^\alpha}(\frac{(U_{i+1}^n - U_i^n)_-}{h} + \frac{(U_i^n - U_{i-1}^n)_+}{h})(\frac{(U_{i+1}^n - U_i^n)_-^2}{h} + \frac{(U_i^n - U_{i-1}^n)_+^2}{h})^{\beta/2-1}$$

$$\frac{\partial F_i}{\partial U_{i+1}^n} = \frac{\nu}{h^2} + \frac{1}{h(c_0+c_1 M_i^{n+1})^\alpha}\frac{(U_{i+1}^n - U_i^n)_-}{h}(\frac{(U_{i+1}^n - U_i^n)_-^2}{h} + \frac{(U_i^n - U_{i-1}^n)_+^2}{h})^{\beta/2-1}$$

Let us denote J_H the Jacobian of $U^n \mapsto (\tilde{H}([\nabla_h U^n]_i), \tilde{M}_i)_{0 \le i < N_h}$ computed at U^n, in the equations above. Since it will be useful in the sequel its coefficients verify :

$$(J_H)_{i,i-1} = -\frac{1}{h(c_0+c_1 M_i^{n+1})^\alpha}\frac{(U_i^n - U_{i-1}^n)}{h} + (\frac{(U_{i+1}^n - U_i^n)_-^2}{h} + \frac{(U_i^n - U_{i-1}^n)_+^2}{h})^{\beta/2-1}$$

$$(J_H)_{i,i} = \frac{1}{h(c_0+c_1 M_i^{n+1})^\alpha}(\frac{(U_{i+1}^n - U_i^n)_-}{h} + \frac{(U_i^n - U_{i-1}^n)_+}{h})(\frac{(U_{i+1}^n - U_i^n)_-^2}{h} + \frac{(U_i^n - U_{i-1}^n)_+^2}{h})^{\beta/2-1}$$

$$(J_H)_{i,i+1} = -\frac{1}{h(c_0+c_1 M_i^{n+1})^\alpha}\frac{(U_{i+1}^n - U_i^n)_-}{h}(\frac{(U_{i+1}^n - U_i^n)_-^2}{h} + \frac{(U_i^n - U_{i-1}^n)_+^2}{h})^{\beta/2-1}$$

3.3 Discrete KFP equation

To define an appropriate discretization of the KFP equation we consider the weak form. For a smooth test function $w \in C^\infty([0,T] \times \Omega)$, it involves, among other terms, the expression :

$$-\int_\Omega \partial_x(H_p(\partial_x u(t,x), m(t,x))m(t,x))w(t,x)\,dx = \int_\Omega m(t,x)H_p(\partial_x u(t,x), m(t,x))\partial_x w(t,x)\,dx,$$

where we used an integration by parts and the Neumann boundary conditions assuming that $H_p(x, 0, m) = 0$. In view of what precedes, it is quite natural to propose the following discrete version of the right-hand side of the equation above :

$$h\sum_{i=0}^{N_h-1} M_i^{n+1}\left[\tilde{H}_{p1}([\nabla_h U^n]_i, M_i^{n+1})\frac{W_{i+1}^n - W_i^n}{h} + \tilde{H}_{p2}([\nabla_h U^n]_i, M_i^{n+1})\frac{W_i^n - W_{i-1}^n}{h}\right],$$

and performing a discrete integration by parts, we obtain the discrete counterpart of the left-hand side of the same equation as follows : $-h\sum_{i=0}^{N_h-1} T_i(U^n, M^{n+1}, M^{n+1})W_i^n$, where T_i is the following discrete transport operator :

$T_i(U, M, \tilde{M}) = \frac{1}{h}\Big[M_i\tilde{H}_{p1}([\nabla_h U]_i, \tilde{M}_i) - M_{i-1}\tilde{H}_{p1}([\nabla_h U]_{i-1}, \tilde{M}_i) + M_{i+1}\tilde{H}_{p2}([\nabla_h U]_{i+1}, \tilde{M}_{i+1}) - M_i\tilde{H}_{p2}([\nabla_h U]_i, \tilde{M}_i)\Big].$

Then, for the discrete version of the second equation in (7), we consider :

$$\begin{cases} (D_t M_i)^n - \nu(\Delta_h M^{n+1})_i - T_i(U^n, M^{n+1}, M^{n+1}) = 0, & 0 < n \leq N_T, \\ M_{-1}^n = M_0^n, \quad M_{N_h}^n = M_{N_h-1}^n, & 0 < n \leq N_T, \\ M_i^0 = \bar{m}_0(x_i), & 0 \leq i < N_h, \end{cases}$$

where U and M are fixed, and for example,

$$\bar{m}_0(x_i) = \frac{1}{h} \int_{|x-x_i| \leq h/2} m_0(x)\, dx,$$

or simply

$$\bar{m}_0(x_i) = m_0(x_i).$$

Here again, the scheme is implicit since the equation is forward in time. But contrary to the HJB scheme, it consists in a forward loop. Starting from time step 0, $M_i^0 = \bar{m}_0(x_i)$ provides an explicit formula for M^0. The n-th step consists in computing M^{n+1} given U^n and M^n. For the implementation, it is important to realize that the matrix of the linear operator $M \mapsto -T(U^n, M, \tilde{M})$ is the conjugate of the Jacobian matrix of the map from $\mathbb{R}^{N_h}$ to $\mathbb{R}^{N_h}$: $\mathbb{R}^{N_h} \ni U \mapsto (\tilde{H}([\nabla_h U]_i, \tilde{M}_i))_{0 \leq i < N_h}$, computed at $U = U^n$ and M^{n+1}.

By replacing finite difference operators by their values in the discrete KFP equation, we obtain :

$$\frac{M_i^{n+1} - M_i^n}{\Delta t} - \nu \frac{M_{i-1}^{n+1} - 2M_i^{n+1} + M_{i+1}^{n+1}}{h^2} - T_i(U^n, M^{n+1}, \tilde{M}^{n+1}) = 0 \tag{9}$$

Using vectors it looks like :

$$\frac{M^{n+1} - M^n}{\Delta t} - \kappa A M^{n+1} + B M^{n+1} = 0 \tag{10}$$

with B the matrix of the linear operator $M \mapsto -T(U^n, M, \tilde{M})$. We recall that B is link to the jacobian matrix of $\tilde{H}([\nabla_h U^n]_i, \tilde{M}_i^{n+1})$ in U^n by : $BM^{n+1} = \frac{\partial \tilde{H}}{\partial U^n}^T M^{n+1} = (J_H)^T M^{n+1}$

By rewriting the vector form of the discrete KFP equation, one can show it is equivalent to :

$$PM^{n+1} = M^n \tag{11}$$

where $P = I - \kappa \Delta t A + \Delta t (J_H)^T$ with A the same matrix as above, J_H the jacobian matrix defined above and I the identity squarred matrix of order N_h defined as follows : $I = \begin{bmatrix} 1 & 0 & 0 & \cdots & 0 \\ 0 & 1 & 0 & \cdots & 0 \\ 0 & 0 & 1 & \cdots & 0 \\ \vdots & \vdots & \vdots & \ddots & 0 \\ 0 & 0 & 0 & 0 & 1 \end{bmatrix}$

3.4 Fixed point iterations for the whole forward-backward system

Let $\mathcal{M}$ stand for the collection $(M^n)_{0,\ldots,N_T}$ and $\mathcal{U}$ stand for the collection $(U^n)_{0,\ldots,N_T}$. The program consists of approximating $(\mathcal{M},\mathcal{U})$ by fixed point iterations involving a relaxation parameter θ. Let θ be a parameter, $0 < \theta < 1$, $\theta = 0.2$ or $\theta = 0.02$ are often sensible choices. Let $(\mathcal{M}^{(k)},\mathcal{U}^{(k)})$ be the running approximation of $(\mathcal{M},\mathcal{U})$. The next approximation $(\mathcal{M}^{(k+1)},\mathcal{U}^{(k+1)})$ is computed as follows :

1. Solve the discrete HJB equation given $\mathcal{M}^{(k)}$. The solution is named $\tilde{\mathcal{U}}^{(k+1)}$.
2. Solve the discrete FP equation given $\tilde{\mathcal{U}}^{(k+1)}$ and $\mathcal{M}^{(k)}$. The solution is named $\tilde{\mathcal{M}}^{(k+1)}$.
3. Set $(\mathcal{M}^{(k+1)},\mathcal{U}^{(k+1)}) = (1-\theta)(\mathcal{M}^{(k)},\mathcal{U}^{(k)}) + \theta(\tilde{\mathcal{M}}^{(k+1)},\tilde{\mathcal{U}}^{(k+1)})$.

These iterations are stopped when the norm of the increment $(\mathcal{M}^{(k+1)},\mathcal{U}^{(k+1)}) - (\mathcal{M}^{(k)},\mathcal{U}^{(k)})$ becomes smaller than a given threshold, say 10^{-6}.

4 Some theoretical results

In this section, we give theoretical results about the finite difference scheme presented above.

4.1 The mass of M^n, i.e., $\sum_{i=0}^{N_h-1} M_i^n$ does not depend on n

We recall that $PM^{n+1} = M^n$. Let $v = (1,1,\ldots,1)^T \in \mathbb{R}^{N_h}$. If we prove that $P^T v = v$, then we are done, as this would imply $v^T P = v^T$ which leads to : $v^T P M^{n+1} = v^T M^{n+1} \Rightarrow v^T M_{n+1} = v^T M_n$, which is exactly what we need to show. We have : $P^T v = (I - \kappa \Delta t A^T + \Delta t J_H) v$. From the expression of J_H, we deduce that the sum its coefficients of over any row is 0, since the diagonal term exactly compensate the sup and the sub diagonal terms. The same applies to the matrix A, so that at row i : $(P^T v)_i = 1 - \kappa \Delta t \cdot 0 + \Delta t \cdot 0 = 1 = v_i$. Hence $P^T v = v$, and we can conclude.

4.2 Uniqueness in the discrete HJB equation, i.e., that given $(M^n)_n$, the sequence $(U^n)_n$ is unique.

Let $(U^n)_n$ and $(V^n)_n$ be two solutions of the HJB equation, namely the first equation in (8) (given $(M^n)_n$). We consider (n_0, i_0) such that : $U_{n_0}^{i_0} - V_{n_0}^{i_0} = \max_{(n,i)}(U_i^n - V_i^n)$. Then :

$$-(D_tU_{i_0})^{n_0} - \nu(\Delta_h U^{n_0})_{i_0} + \tilde{H}([\nabla_h U^{n_0}]_{i_0}, M_{i_0}^{n_0+1}) = -(D_tV_{i_0})^{n_0} - \nu(\Delta_h V^{n_0})_{i_0} + \tilde{H}([\nabla_h V^{n_0}]_{i_0}, M_{i_0}^{n_0+1}).$$

Rearranging terms :

$$\tilde{H}([\nabla_h U^{n_0}]_{i_0}, M_{i_0}^{n_0+1}) - \tilde{H}([\nabla_h V^{n_0}]_{i_0}, M_{i_0}^{n_0+1}) = (D_tU_{i_0})^{n_0} + \nu(\Delta_h U^{n_0})_{i_0} - (D_tV_{i_0})^{n_0} - \nu(\Delta_h V^{n_0})_{i_0}. \tag{12}$$

Knowing that $U_{i_0})^{n_0} - V_{i_0})^{n_0}$ is the largest difference, we have by definition of D_t and Δ_h :

$$\begin{cases} (D_tU_{i_0})^{n_0} - (D_tV_{i_0})^{n_0} = \frac{1}{\Delta t}(-(U_{i_0}^{n_0} - V_{i_0}^{n_0}) + (U_{i_0}^{n_0+1} - V_{i_0}^{n_0+1}) \leq 0 \\ (\nu\Delta_h U_{i_0})^{n_0} - (\nu\Delta_h V_{i_0})^{n_0} = \frac{\nu}{h^2}((U_{i_0+1}^{n_0} - V_{i_0+1}^{n_0}) + 2(U_{i_0}^{n_0} - V_{i_0}^{n_0}) + (U_{i_0-1})^{n_0} - V_{i_0-1})^{n_0}) \leq 0 \end{cases}$$

Hence, $\tilde{H}([\nabla_h U^{n_0}]_{i_0}, M_{i_0}^{n_0+1}) \leq \tilde{H}([\nabla_h V^{n_0}]_{i_0}, M_{i_0}^{n_0+1})$. Futhermore :

$$\begin{cases} (DU^{n_0})_{i_0} - (DV^{n_0})_{i_0} = \frac{1}{h}((U_{i_0+1}^{n_0} - V_{i_0+1}^{n_0}) - (U_{i_0}^{n_0} - V_{i_0}^{n_0})) \leq 0 & (a) \\ (DU^{n_0})_{i_0-1} - (DV^{n_0})_{i_0-1} = \frac{1}{h}((U_{i_0}^{n_0} - V_{i_0}^{n_0}) - (U_{i_0-1}^{n_0} - V_{i_0-1}^{n_0})) \geq 0 & (b) \end{cases}$$

Since $\tilde{H}$ is non-decreasing in its second argument and non-increasing in its first argument, it follows that :

$$\tilde{H}([\nabla_h U^{n_0}]_{i_0}, M_{i_0}^{n_0+1}) \leq \tilde{H}([\nabla_h V^{n_0}]_{i_0}, M_{i_0}^{n_0+1}).$$

i.e

$$\begin{aligned} \tilde{H}((DU^{n_0})_{i_0}, (DU^{n_0})_{i_0-1}, M_{i_0}^{n_0+1}) &\leq \tilde{H}((DV^{n_0})_{i_0}, (DV^{n_0})_{i_0-1}, M_{i_0}^{n_0+1}) \\ &\leq \tilde{H}((DU^{n_0})_{i_0}, (DV^{n_0})_{i_0-1}, M_{i_0}^{n_0+1}) \quad \text{using (a) and the non-increasing property} \\ &\leq \tilde{H}((DU^{n_0})_{i_0}, (DU^{n_0})_{i_0-1}, M_{i_0}^{n_0+1}) \quad \text{using (b) and the non-decreasing property} \end{aligned}$$

We conclude that $\tilde{H}(x_{i_0}, (DU^{n_0})_{i_0}, (DU^{n_0})_{i_0-1}) = \tilde{H}(x_{i_0}, (DV^{n_0})_{i_0}, (DV^{n_0})_{i_0-1})$. by the non-increasing property and by the non-decreasing property. We conclude that :

$$\tilde{H}((DU^{n_0})_{i_0}, (DU^{n_0})_{i_0-1}, M_{i_0}^{n_0+1}) = \tilde{H}((DV^{n_0})_{i_0}, (DV^{n_0})_{i_0-1}, M_{i_0}^{n_0+1}).$$

By take into account (a) and (b) in (12) this result show that a sum of negative numbers is equal to 0. Which means that all of the terms of the sum are identically null. (12) then looks like :

$$(D_tU_{i_0})^{n_0} - (D_tV_{i_0})^{n_0} = 0, \quad (\nu\Delta_h U_{i_0})^{n_0} - (\nu\Delta_h V_{i_0})^{n_0} = 0$$

From what we said above, instead of inequality we have equality in both (a) and (b). We then conclude that $\max_{(n,i)}(U_i^n - V_i^n)$ is also reached on the adjacent points of (i_0, n_0), namely (i_0+1, n_0), (i_0-1, n_0) and (i_0, n_0+1). The arguments developed above then propagate iteratively until we reach the boundary condition $U_i^{N_T} = V_i^{N_T} = \varphi(M_i^{N_T})$ for all $0 \leq i < N_h$, which implies that $\max_{(i,n)} U_i - V_i = 0$. Hence, $U = V$, and the solution to the discrete HJB equation is unique.

4.3 Uniqueness in the discrete KFP equation, i.e., that given $(U^n)_n$, the sequence $(M^n)_n$ is unique

We know that finding M^{n+1} given M^n and $(U_n)_n$ is equivalent to solving : $PM^{n+1} = (I - \kappa\Delta t A + \Delta t(J_H)^T)M^{n+1} = M^n$. We will show that P^T has the M-matrix property :

1. First $P^T_{i,i} = P_{i,i} > 0$ for all $0 \leq i < N_h$. Indeed :

$$P_{i,i} = 1 - \kappa\Delta t \cdot (-1 \text{ or } -2) + \Delta t \cdot (J_H)^T_{i,i} \geq 1 + \kappa\Delta t \cdot + \Delta t \cdot (J_H)^T_{i,i},$$

which is strictly greater than 0 since $(J_H)^T_{i,i} \geq 0$ for all i .

2. For $j \neq i$, we have $P^T_{i,j} \leq 0$:

$$P^T_{i,j} = -\kappa\Delta t + \Delta t \cdot (J_H)_{i,j} \leq 0.$$

since $(J_H)^T_{i,j} \leq 0$ for all $j \neq i$.

3. The sum of coefficients over any row of J_H is null, leading to :

$$\sum_{j=0}^{N_h-1} P^T_{i,j} = 1 - \nu\Delta t \cdot 0 + \Delta t \cdot 0 > 0.$$

Therefore, P^T has the M-property, so it is invertible, and then also P is invertible. Hence, the system $PM^{n+1} = M^n$ has a unique solution. We could make the demonstration shorter by just observing that $-\kappa\Delta t A$ and $\Delta t(J_H)^T$ are tridiagonal M-matrix.

4.4 If M^0 is positive, then M^n is positive for all n

We will prove this by induction. Assume that M^0 is positive, then $PM^1(= M^0)$ is also positive. Reminding from the above section, that P^T is an M-matrix. It follows that (P^T) is monotone, and consequently P is monotone. This implies that M^1 is positive. Thus, assume M^n is positive at rank n using the equality $PM^{n+1} = M^n$ and the fact that P is Monotone, we deduce that M^{n+1} is positive. Hence, $M^0 \geq 0$ implies that M^n is positive for all n.

5 Mean Field Games Simulation

This section explores the result we came up with after performing simulation with differents sets of parameters. We considered the following data

- $\Omega =]0,1[, \quad T = 1$
- $g(x) = 0$
- H_0 is defined in section 2 and the discrete Hamiltonian is given in subsection 3.1 . We try the following sets of parameters :
  (a) $\beta = 2, \quad c_0 = 0.1, \quad c_1 = 1, \quad \alpha = 0.5, \quad \sigma = 0.02$
  (b) $\beta = 2, \quad c_0 = 0.1, \quad c_1 = 5, \quad \alpha = 1, \quad \sigma = 0.02$
  (c) $\beta = 2, \quad c_0 = 0.01, \quad c_1 = 2, \quad \alpha = 1.2, \quad \sigma = 0.1$
  (d) $\beta = 2, \quad c_0 = 0.01, \quad c_1 = 2, \quad \alpha = 1.5, \quad \sigma = 0.2$
  (e) $\beta = 2, \quad c_0 = 1, \quad c_1 = 3, \quad \alpha = 2, \quad \sigma = 0.002$
- $\tilde{f}(m(x)) = \frac{m(x)}{10}$
- $\phi(x, m) = -\exp(-40(x-0.7)^2)$
- $m_0(x) = \sqrt{\frac{300}{\pi}} \exp(-300(x-0.2)^2)$.
- $N_h = 201, \quad N_T = 100$.
- The parameter θ is chosen in such a way that the fixed point method converges. Depending on the case of interest, the good values of θ may lie in the interval $[0.001, 0.2]$.
- Stopping criteria in the Newton method : 10^{-10}.
- Stopping criteria in the fixed point method : not larger than 2×10^{-5} (with norms normalized so that $\|(1, \ldots, 1)\| = 1$).

For each set of parameters we plot the contour lines of u and m in the plane (x, t) and we realised animations showing the evolution of u and m with respect to time. The figures below shows the result of the simulations.

5.1 Figure 1 : $\beta = 2$, $c_0 = 0.1$, $c_1 = 1.0$, $\alpha = 0.5$, $\sigma = 0.02$

Contour of u (value function) : The value function u increases steadily over time, transitioning from negative values (around -0.96) to nearly positive values. This growth is consistent with an optimal control problem with a congestion effect. The low value of $c_1 = 1.0$ limits the effect of density m on motion cost. This results in moderate growth of u in regions where density m is high.

Contour of m (population density) : The density m is initially concentrated around $x = 0.2$, which corresponds to the initial condition $m_0(x) = \sqrt{300/\pi}\exp(-300(x-0.2)^2)$. With $c_1 = 1.0$ and $\alpha = 0.5$, congestion effects are very limited. The density m remains weakly concentrated over time, which is consistent with a moderate movement cost in relatively populated areas. The diffusion is moderate ($\sigma = 0.02$), allowing the density to disperse rather quickly from its initial value without remaining concentrated for long in specific locations.

5.2 Figure 2 : $\beta = 2$, $c_0 = 0.1$, $c_1 = 5.0$, $\alpha = 1.0$, $\sigma = 0.02$

Contour of u (value function) : The value function u increases steadily over time, transitioning from negative values (around -0.90) to positive values (up to 0.30). The higher value of $c_1 = 5.0$ compared to Figure 1 amplifies the effect of density m on movement cost. This results in a more pronounced growth of u over time in regions where density m is high.

Contour of m (population density) : The density m is initially concentrated around $x = 0.2$ and remains so over time, with $c_1 = 5.0$ and $\alpha = 1.0$, which make congestion effects quite significant. The density m stays concentrated in certain regions, even over time, which is consistent with a high movement cost in densely populated areas. The diffusion is moderate ($\sigma = 0.02$), allowing the density to disperse gradually while maintaining regions of high concentration.

5.3 Figure 3 : $\beta = 2$, $c_0 = 0.01$, $c_1 = 2.0$, $\alpha = 1.2$, $\sigma = 0.1$

Contour of u (value function) : The value function u grows more rapidly than in Figure 2, transitioning from negative values (down to -1.0) to values close to 0. The increase in α compared to Figure 2 (from 1.0 to 1.2) strengthens congestion effects, leading to a faster growth of u.

Contour of m (population density) : The density m is initially concentrated around $x = 0.2$, but disperses more quickly than in Figure 2, due to the higher value of $\sigma = 0.1$. Despite the faster diffusion, congestion effects ($c_1 = 2.0$ and $\alpha = 1.2$) maintain high concentration areas in certain regions.

5.4 Figure 4 : $\beta = 2$, $c_0 = 0.01$, $c_1 = 2.0$, $\alpha = 1.5$, $\sigma = 0.2$

Contour of u (value function) : The value function u grows even faster than in Figure 3, with values ranging from -1.000 to 0. This is due to the increase in $\alpha = 1.5$, which amplifies congestion effects. The greater diffusion ($\sigma = 0.2$) also contributes to the rapid growth of u, as it allows density m to disperse more quickly, influencing movement cost.

Contour of m (population density) : The density m is initially concentrated around $x = 0.2$, but disperses even faster than in Figure 3, due to the higher value of $\sigma = 0.2$. Congestion effects ($c_1 = 2.0$ and $\alpha = 1.5$) are very pronounced, maintaining high concentration areas despite the diffusion. However, the concentration is lower than in Figure 3.

5.5 Figure 5 : $\beta = 2$, $c_0 = 1$, $c_1 = 3.0$, $\alpha = 2.0$, $\sigma = 0.002$

Contour of u (value function) : The value function u grows faster than in the previous graphs, with values ranging between -1.0 and 0.6. This is due to the higher value of $c_0 = 1$, which reduces the effect of density m on movement cost. With the high value of α, the growth of u is more pronounced than in previous graphs, as $c_0 = 1$ mitigates congestion effects.

Contour of m (population density) : The density m is initially concentrated around $x = 0.2$, but disperses much more slowly than in previous graphs, due to the low value of $\sigma = 0.002$. Congestion effects ($c_1 = 3.0$ and $\alpha = 2.0$) are very pronounced, maintaining high concentration areas around the initial value, which persist in space and time. The diffusion is very low ($\sigma = 0.002$), explaining why the density disperses very slowly while sustaining regions of very high concentration.

Conclusion : The differences between the figures are mainly explained by variations in the parameters c_0, c_1, α, and σ. These parameters influence both the growth of the value function u and the dispersion of density m. Congestion effects are particularly noticeable in graphs where c_1 and α are high, while diffusion is more or less pronounced depending on the value of σ. These observations are consistent with theoretical expectations.

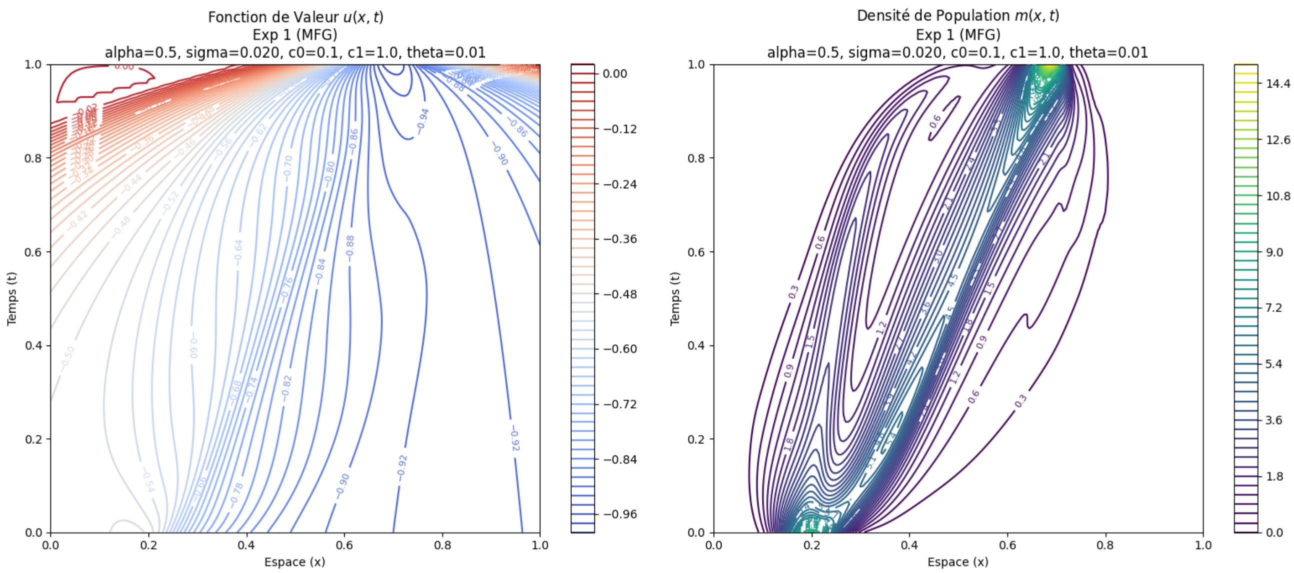

FIGURE 1 – Contour lines of u and m in the example (a) described above

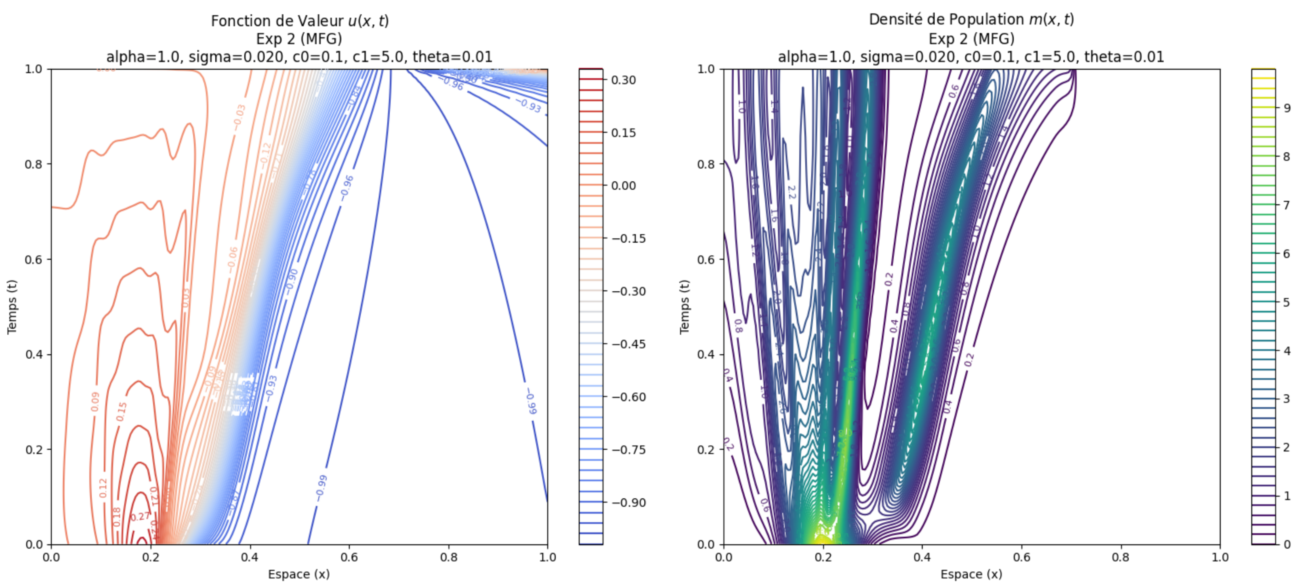

FIGURE 2 – Contour lines of u and m in the example (b) described above

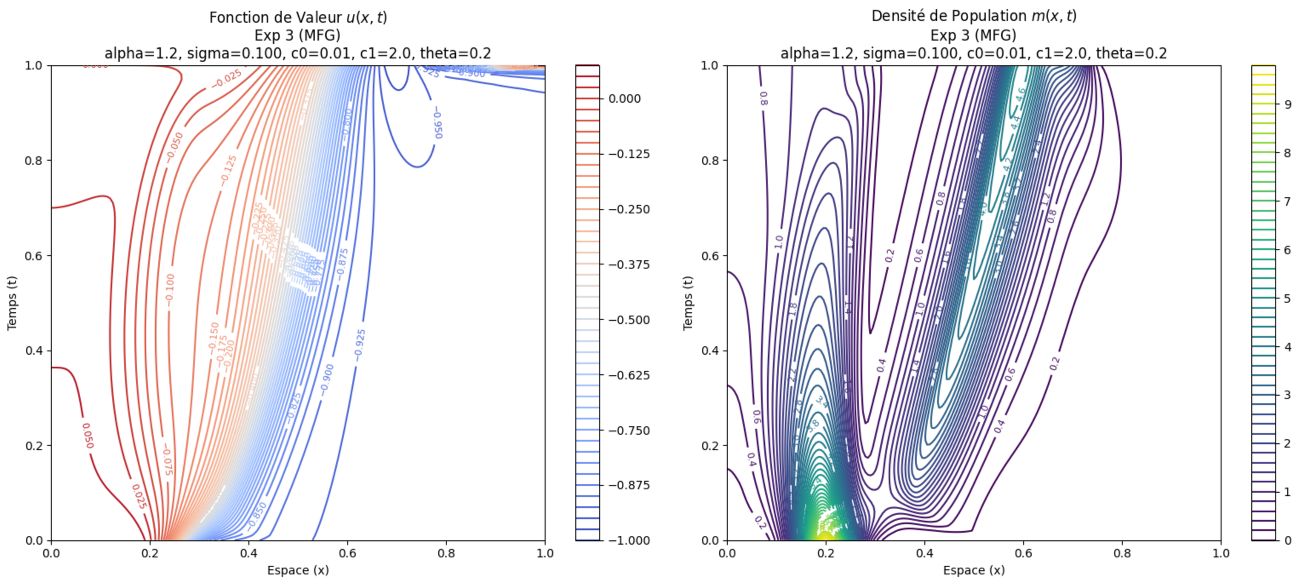

FIGURE 3 – Contour lines of u and m in the example (c) described above

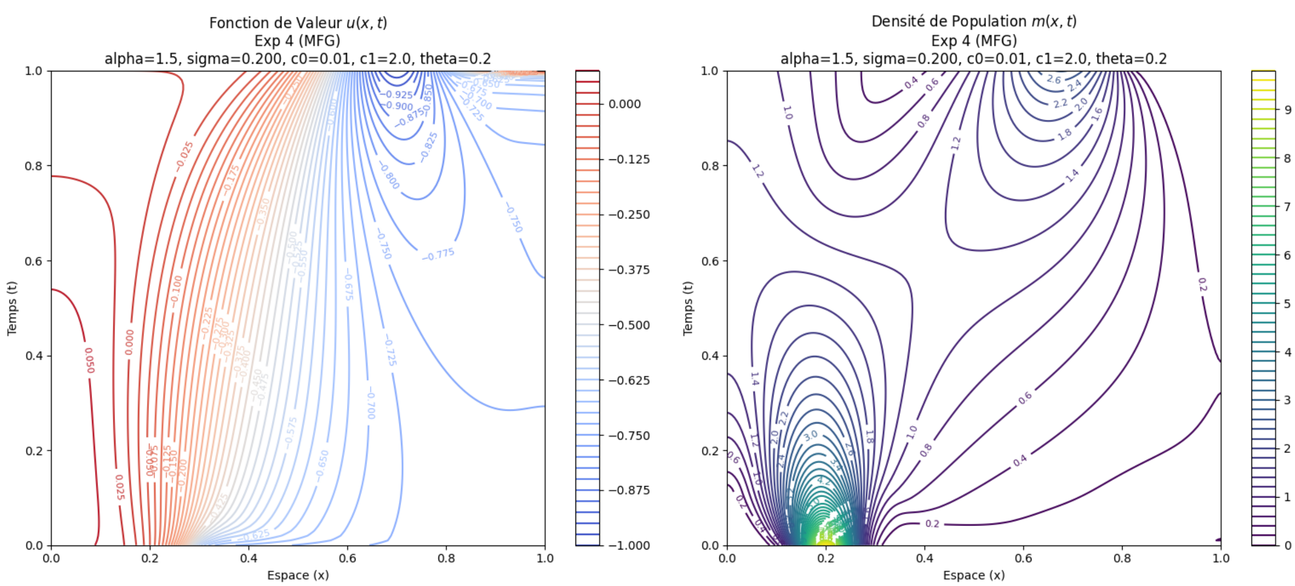

FIGURE 4 – Contour lines of u and m in the example (d) described above

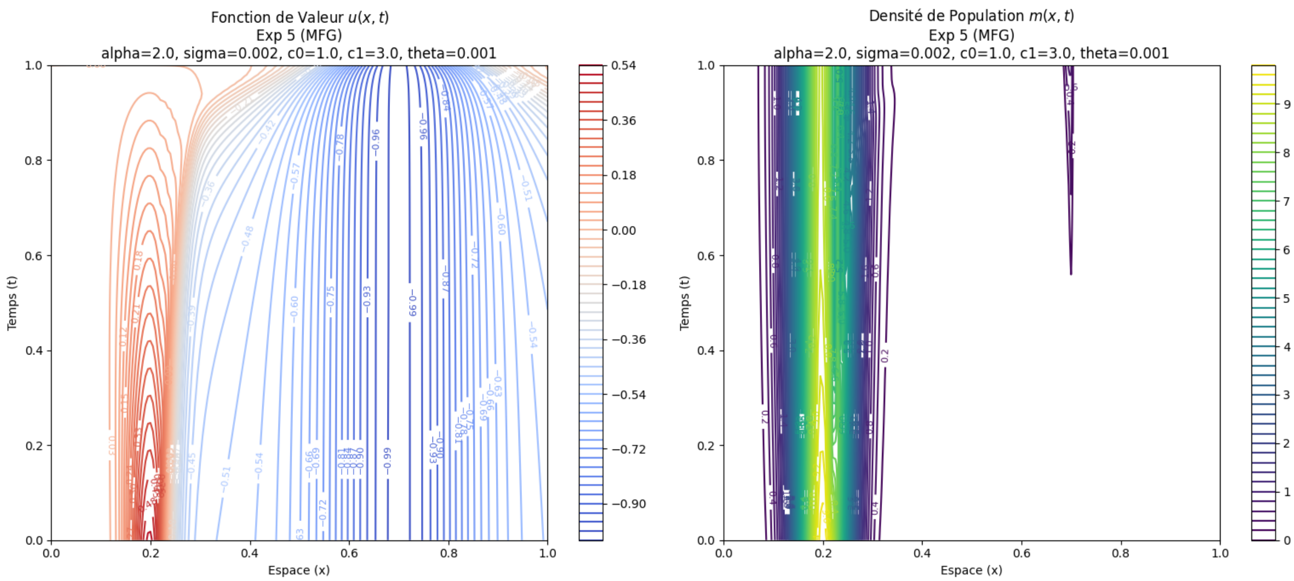

FIGURE 5 – Contour lines of u and m in the example (e) described above

6 Mean field control

As mentioned in the introduction, the theory of mean field games allows one to study Nash equilibria in games with a number of players tending to infinity. In such models, the players are selfish and try to minimize their own individual cost. Another kind of asymptotic regime is obtained by assuming that all the agents use the same distributed feedback strategy and by passing to the limit as $N \to \infty$ before optimizing the common feedback. This is the situation when a planner controls a crowd of robots which interact via aggregate global or local quantities, in order to optimize a global criterion. For a fixed common feedback strategy, the asymptotic behavior is given by the McKean-Vlasov theory : the dynamics of a representative agent is found by solving a stochastic differential equation with coefficients depending on a mean field, namely the statistical distribution of the states, which may also affect the objective function.

Since the feedback strategy is common to all agents, perturbations of the latter affect the mean field (whereas in a mean field game, the other players' strategies are fixed when a given player chooses her strategy). Then, having each agent optimize her objective function amounts to solving a control problem driven by the McKean-Vlasov dynamics. The latter is named control of McKean-Vlasov dynamics or mean field control. Besides the aforementioned interpretation as a social optimum in collaborative games with a number of agents growing to infinity, mean field control problems have also found applications in finance and risk management for problems in which the distribution of states is naturally involved in the dynamics or the cost function.

Mean field control problems lead to a system of forward-backward PDEs which has some features similar to the MFG system, but which can always be seen as the optimality conditions of a minimization problem. Using the same model of congestion as above, the system of PDEs that arises is the following :

$$\begin{cases} -\frac{\partial u}{\partial t}(t,x) - \nu \frac{\partial^2 u}{\partial x^2}(t,x) + \frac{1}{\beta}\frac{|\nabla u(t,x)|^\beta|}{(c_0+c_1 m(t,x))^\alpha} - \frac{c_1\alpha}{\beta}\frac{m(t,x)|\nabla u(t,x)|^\beta}{(c_0+c_1 m(t,x))^{\alpha+1}} & \\ = g(x) + \tilde{f}_0(m(t,x)) + m(t,x)\tilde{f}_0'(m(t,x)), & \text{in } [0,T) \times \Omega, \\ \frac{\partial m}{\partial t}(t,x) - \nu \frac{\partial^2 m}{\partial x^2}(t,x) - \frac{\partial}{\partial x}\left(\frac{m(t,\cdot)}{(c_0+c_1 m(t,\cdot))^\alpha} \left|\frac{\partial u}{\partial x}(t,\cdot)\right|^{\beta-2} \frac{\partial u}{\partial x}(t,\cdot)\right)(x) = 0, & \text{in } (0,T] \times \Omega, \\ \frac{\partial u}{\partial x}(t,0) = \frac{\partial u}{\partial x}(t,1) = 0, & \text{on } (0,T), \\ \frac{\partial m}{\partial x}(t,0) = \frac{\partial m}{\partial x}(t,1) = 0, & \text{on } (0,T) \\ u(T,x) = \phi(x), \quad m(0,x) = m_0(x), & \text{in } \Omega. \end{cases}$$

It can be proved that if $\beta > 1$, $0 \leq \alpha < 1$ and $\tilde{f}_0$ is convex, then there is a unique solution.

We compare and comment the result of the simulation of MFG and mean field control. The parameters used are those from case (a) in section 5 : $\beta = 2$, $c_0 = 0.1$, $c_1 = 1$, $\alpha = 0.5$, $\sigma = 0.02$.

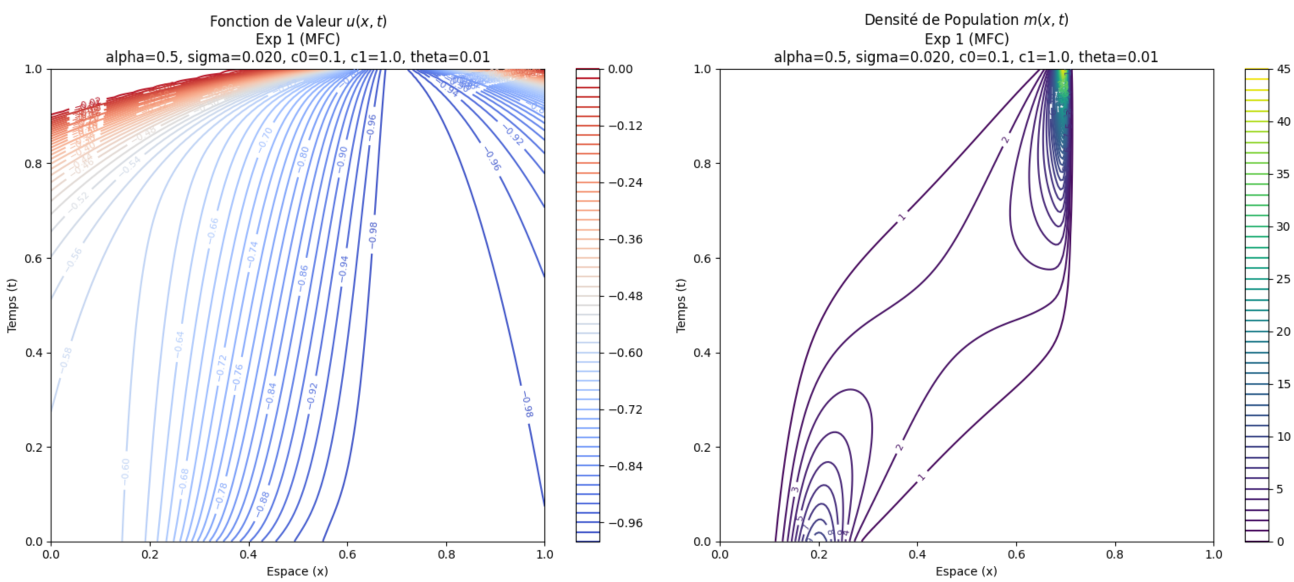

FIGURE 6 – Contour lines of u and m in the example (a) in case of MFC

6.1 Critical Comparison : MFG vs MFC (Experiment 1)

The comparative analysis of Experiment 1 ($\alpha = 0.5, \sigma = 0.02, c_0 = 0.1, c_1 = 1.0$) underscores the fundamental divergences between a decentralized system (MFG) and a system coordinated by a central planner (MFC).

6.1.1 Analysis of population density $m(x,t)$

The most striking difference lies in the magnitude and structure of the mass concentration :

— **Concentration and Coordination :** In **MFG** mode, the maximum density peaks at approximately 14.4. The population moves toward the target ($x \approx 0.7$) in a relatively dispersed manner. Conversely, in **MFC** mode, the density peaks at approximately 45.0. The central planner imposes a much narrower and more coherent trajectory.

— **Efficiency vs. Dispersion :** The social strategy (MFC) appears to "sacrifice" spreading in order to force a massive and rapid convergence toward the objective. While agents in the MFG are subject to diffusion ($\sigma = 0.02$) individually, the MFC compensates for this noise with strict global control, thereby minimizing the total transport cost for the entire population.

6.1.2 Analysis of the value function $u(x,t)$

The potential field u reflects the difference in the system's governance :

— **Anticipation of Congestion :** In the **MFC** case, the value function incorporates the marginal cost that an agent imposes on the collective. Graphically, this results in more vertical level lines at the beginning of the simulation, creating a proactive "navigation corridor."

— **Local Reactivity :** In **MFG**, the level lines exhibit a smoother curvature. Agents react to density in a reactive rather than proactive manner, leading to a Nash equilibrium that is globally less efficient than the social optimum.

Conclusion : For this set of parameters, the social optimum (MFC) prioritizes a massive concentration on the target to optimize the global criterion. The Nash equilibrium (MFG) illustrates a lack of coordination where individual freedom of movement results in increased dispersion and a significantly lower peak density.

Références

[1] Jean-Michel Lasry and Pierre-Louis Lions. Jeux à champ moyen. i – le cas stationnaire. *C.R.Math.Acad.Sci.Paris*, 343(2006) :pp. 619–625, 2006.

[2] Jean-Michel Lasry and Pierre-Louis Lions. Jeux à champ moyen. ii. horizon fini et contrôle optimal. *C.R.Math.Acad.Sci.Paris*, 343(2006) :pp. 679–684, 2006.

[3] Y.Achdou and I.Capuzzo-Dolcetta. Mean field games : numerical methods. *SIAMJ.Numer.Anal.*, 48(2010) :pp. 1136—-1162, 2010.